Supporting Information

Lewis *et al.* 10.1073/pnas.0802501105

SI Text: Notes on Glacial Modeling

To estimate the temperature at which glaciers within the Olympus Range became cold-based, we modeled a glacier for which we have a mid-Miocene configuration based on mapped moraines and drift limits. The glacier was just under 11 km in length, and no more than 100 m in thickness (Fig. S2). The uncertainties in paleoclimate and long-term (>10,000 years) stability of glacier margins make appropriate a steady-state, thermomechanically coupled model with higher-order stress treatments (full Stokes equations are solved in the x–z plane) (1). The surface boundary was stress-free, and an adiabatic lapse rate and a temperature at sea level specified the surface temperature. For basal boundary conditions, we specified no basal sliding and used regional estimates (2) of 68 $mW{\cdot}m^{-2}$ for geothermal heat flux. To determine the surface temperature corresponding to the transition from warm- to cold-based conditions, the inverse model was used, altering temperature at sea level until the glacial bed exceeded the pressure melting point.

The thermodynamic model is accounting for strain heating, temperature advection due to ice flow, and geothermal heating. It is neglecting the contributions of surface melt water and heats of fusion that would arise as the temperatures increase. At this time, we know of no physics-based models for this process. We maintain that our approach is a good first-order approximation of the point at which the cold- to wet-based transition occurs due to the high rates of evaporation resulting from strong katabatic winds in the area. Hence, we do not anticipate that surface melt played a significant role in the heat budget of this glacier.

Model results (Fig. S2) show that basal ice conditions would have been sensitive to ice surface temperature (annual average air temperature) and geothermal heat flow, but insensitive to accumulation rates. The maximum mean surface temperature that maintains cold-based conditions is −3°C, indicating that the contribution of ice flow and deformation heating in this glacier is ≈3°C of heating.

1. Johnson JV, Willenbring JK (2007) Modeling long-term stability of the Ferrar Glacier, East Antarctica: Implications for interpreting cosmogenic nuclide inheritance. *J Geophys Res* 112:F03S30.

2. Llubes M, Lanseau C, Rémy F (2006) Relations between basal condition, subglacial hydrological networks and geothermal heat flux in Antarctica. *Earth Planet Sci Lett* 241:655–662.

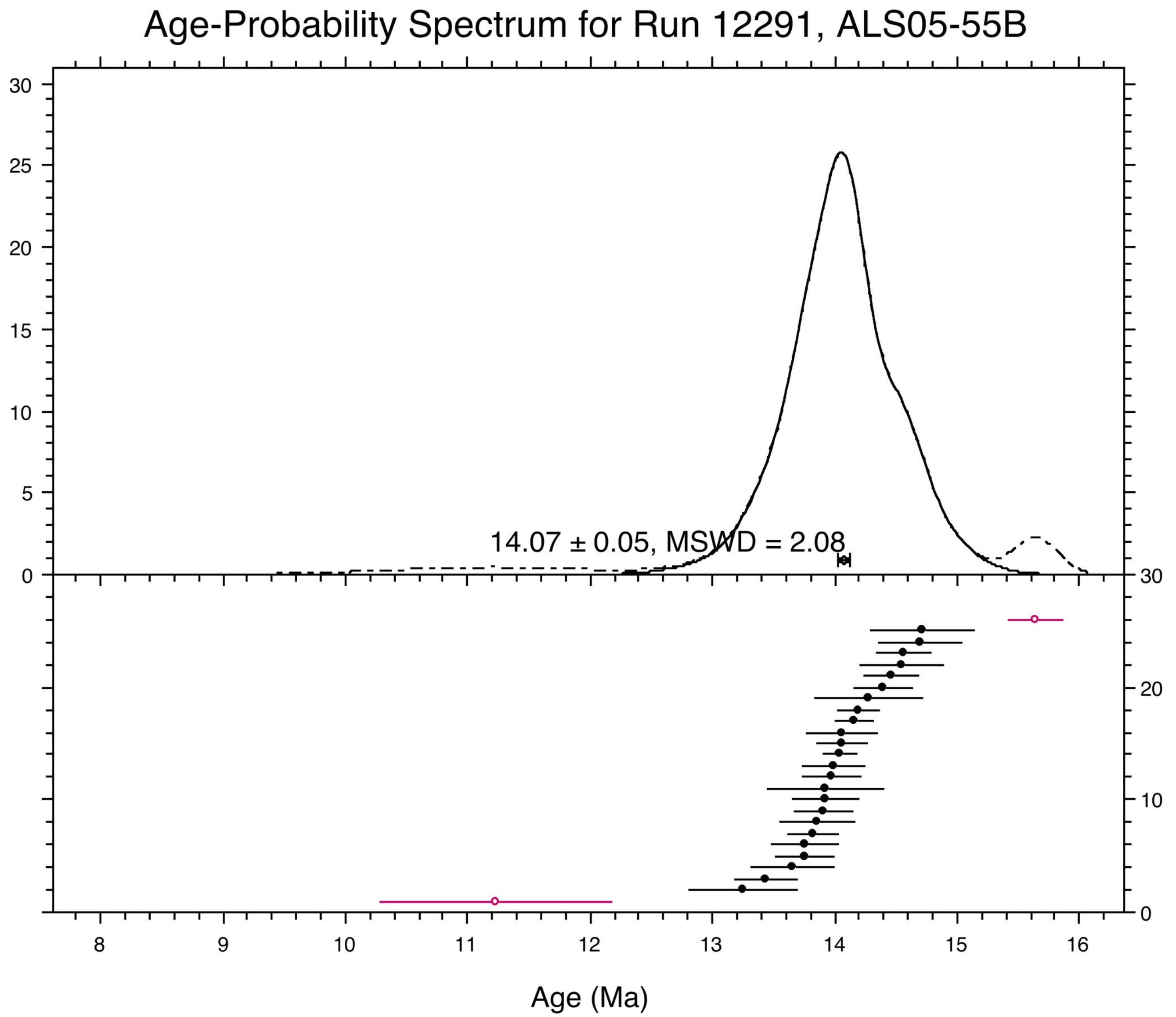

Fig. S1. Age probability spectrum of single-crystal analyses. Results $>3\ \sigma$ from the mean (shown in red) are excluded from the age calculation.

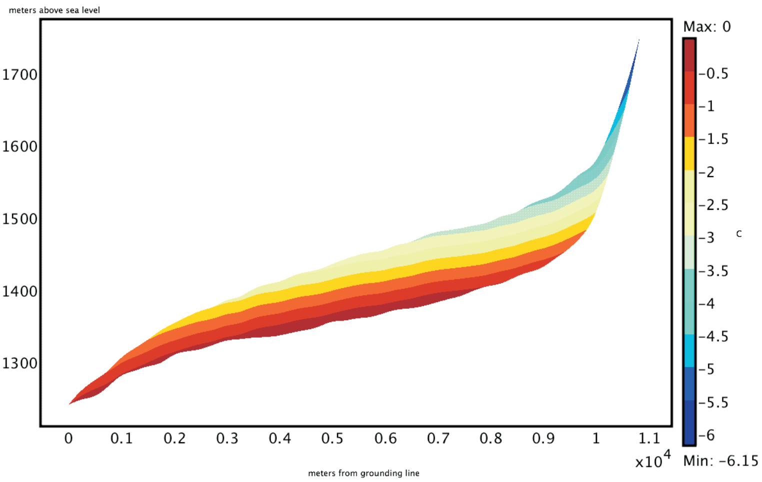

Fig. S2. Homologous temperatures for Olympus Range glacier at the transition between cold- and warm-based conditions.

Table S1. $^{40}Ar/^{39}Ar$ Analytical data for ash sample ALS 05-55B

	Relative Isotopic Abundances										Derived Results							Inverse Isochron Data				
Lab ID#	^{40}Ar	±1σ	^{39}Ar	±1σ	^{38}Ar	±1σ	^{37}Ar	±1σ	^{36}Ar	±1σ	^{39}Ar Mol × 10^{-14}	Ca/K	±1σ	$\%^{40}Ar^{*}$	Age (Ma)	±1σ	w/±*J* ±1σ	$^{36}Ar/^{40}Ar$	±%1σ	$^{39}Ar/^{40}Ar$	±%1σ	$^{36}Ar/^{39}Ar$ Er. Corr.
ALS05-55B																						
12291-01	3.9953	0.0076	1.1737	0.0036	0.0146	0.0007	0.022	0.0014	0.0023	0.0002	0.16	0.036648	0.00228	83.3	13.43983	0.211651	0.21	0.00057	7.57	0.29384	0.39	0.0455
12291-02	3.3298	0.0052	0.9982	0.0023	0.0119	0.0005	0.061	0.0017	0.0013	0.0001	0.14	0.119709	0.00326	88.5	13.99407	0.208714	0.21	0.00039	11.20	0.29984	0.31	0.0312
12291-03	3.0894	0.0065	0.8666	0.0023	0.011	0.0006	0.0181	0.0013	0.0018	0.0001	0.12	0.04085	0.0029	83.2	14.06932	0.24266	0.24	0.00057	8.35	0.28057	0.36	0.0436
12291-04	3.5571	0.008	1.1426	0.0024	0.0148	0.0007	0.0373	0.0016	0.0008	0.0002	0.16	0.064	0.00262	93.2	13.7505	0.209006	0.21	0.00023	20.18	0.32130	0.34	0.0191
12291-05	2.0409	0.0061	0.5211	0.0019	0.007	0.0005	0.0118	0.0012	0.0016	0.0001	0.07	0.044258	0.00454	76.8	14.26576	0.406671	0.41	0.00078	9.29	0.25537	0.50	0.0418
12291-06	*0.878*	*0.005*	*0.226*	*0.001*	*0.003*	*4E-04*	*0.003*	*0.001*	*0.001*	*1E-04*	*0.03*	*0.02583*	*0.0091*	*61.0*	*11.2349*	*0.90491*	*0.91*	*0.00132*	*12.54*	*0.25771*	*0.81*	*0.0386*
12291-08	5.8385	0.0071	1.8704	0.0035	0.0227	0.0008	0.1233	0.0027	0.0011	0.0001	0.25	0.129215	0.00276	94.8	14.0358	0.108451	0.11	0.00017	13.36	0.32042	0.25	0.0261
12291-09	5.3063	0.0078	1.6712	0.0041	0.02	0.0006	0.056	0.0022	0.001	0.0002	0.23	0.065729	0.00257	94.3	14.19267	0.133859	0.14	0.00019	14.65	0.31501	0.31	0.0233
12291-10	2.5506	0.0055	0.7861	0.0023	0.0097	0.0004	0.04	0.002	0.0006	0.0001	0.11	0.099677	0.00486	93.5	14.38995	0.214375	0.22	0.00022	20.88	0.30828	0.39	0.0174
12291-11	2.8116	0.0061	0.9302	0.0023	0.0113	0.0004	0.0372	0.0021	0.0002	0.0001	0.13	0.07838	0.0043	97.6	13.98187	0.19305	0.19	0.00008	53.55	0.33092	0.36	0.0070
12291-12	2.7134	0.0052	0.8096	0.0018	0.0094	0.0004	0.0294	0.0021	0.0012	0.0001	0.11	0.071216	0.00506	86.6	13.76017	0.240736	0.24	0.00045	11.09	0.29843	0.32	0.0330
12291-13	1.8199	0.0057	0.4803	0.0022	0.0072	0.0004	0.0192	0.0019	0.0011	0.0001	0.07	0.078408	0.0075	81.9	14.7037	0.391078	0.39	0.00061	11.70	0.26395	0.58	0.0317
12291-14	2.2226	0.0053	0.7377	0.0023	0.009	0.0004	0.0187	0.002	0.0002	0.0001	0.10	0.049712	0.00519	97.4	13.92027	0.242207	0.24	0.00009	64.66	0.33200	0.42	0.0057
12291-15	2.2261	0.006	0.6353	0.0023	0.0077	0.0004	0.0347	0.002	0.0009	0.0001	0.09	0.107114	0.00617	88.5	14.70285	0.29231	0.29	0.00039	14.87	0.28546	0.48	0.0252
12291-16	4.2104	0.0073	1.1825	0.0034	0.0155	0.0006	0.0335	0.0023	0.0021	0.0002	0.16	0.05547	0.00383	85.7	14.46009	0.189844	0.19	0.00049	7.51	0.28091	0.36	0.0456
12291-17	1.8329	0.005	0.5613	0.0019	0.0073	0.0004	0.0171	0.0019	0.0007	0.0001	0.08	0.059529	0.00656	88.2	13.65142	0.314354	0.32	0.00040	16.82	0.30631	0.46	0.0227
12291-18	*3.25*	*0.006*	*0.978*	*0.003*	*0.011*	*5E-04*	*0.053*	*0.002*	*9E-05*	*1E-04*	*0.13*	*0.10528*	*0.0046*	*99.3*	*15.6446*	*0.18016*	*0.18*	*0.00002*	*154.71*	*0.30088*	*0.38*	*0.0023*
12291-19	3.8434	0.0074	1.1773	0.0025	0.0138	0.0004	0.0204	0.002	0.0014	0.0001	0.16	0.033987	0.00335	89.3	13.82928	0.161797	0.16	0.00036	9.41	0.30639	0.31	0.0392
12291-20	3.5478	0.007	1.1552	0.0032	0.0148	0.0005	0.0267	0.002	0.0004	0.0001	0.16	0.045308	0.00334	96.5	14.05335	0.168031	0.17	0.00012	31.60	0.32570	0.37	0.0113
12291-21	1.9616	0.0058	0.5788	0.0021	0.0075	0.0004	0.0425	0.0022	0.0006	0.0001	0.08	0.14374	0.00748	90.5	14.53937	0.303595	0.30	0.00032	19.32	0.29512	0.49	0.0202
12291-22	2.7875	0.0056	0.9133	0.0022	0.0112	0.0005	0.0285	0.002	0	0.0001	0.12	0.06122	0.00423	100.6	14.55723	0.186502	0.19	0.00000	0.00	0.32773	0.34	0.0018
12291-23	5.3514	0.0088	1.6859	0.0031	0.0196	0.0005	0.0661	0.0028	0.0011	0.0001	0.23	0.076857	0.00327	94.1	14.16381	0.117091	0.12	0.00020	12.43	0.31512	0.27	0.0291
12291-24	2.897	0.0057	0.9341	0.0024	0.0114	0.0005	0.0753	0.0024	0.0005	0.0001	0.13	0.157882	0.00501	94.6	13.91165	0.203266	0.20	0.00018	24.93	0.32252	0.35	0.0145
12291-25	1.6332	0.0048	0.4508	0.0018	0.0062	0.0004	0.0506	0.0024	0.0013	0.0001	0.06	0.219863	0.01014	77.1	13.25407	0.415407	0.42	0.00077	10.42	0.27607	0.52	0.0362
12291-26	1.2013	0.0075	0.3927	0.0019	0.0051	0.0004	0.0149	0.002	0.0002	0.0001	0.05	0.074349	0.00966	96.0	13.92269	0.435891	0.44	0.00014	72.43	0.32697	0.82	0.0085
12291-27	2.3901	0.0064	0.7322	0.0019	0.0099	0.0004	0.0277	0.0012	0.0009	0.0001	0.10	0.074142	0.00307	89.5	13.85969	0.273015	0.27	0.00035	16.53	0.30642	0.40	0.0241

All crystals: 14.14+/-0.05, MSWD = 5.23

Filtered (italicized crystals omitted) 14.07+/-0.05, MSWD = 2.08, elimination criterion = 2

Volcanic ash was collected separately and placed in sealed whirl-pack bags for transport to the laboratory. Individual sanidine crystals used for $^{40}Ar/^{39}Ar$ dating were handpicked from aliquots washed in deionized water; crystal selection was made on the basis of crystal habit, cleavage, and size. Crystals were co-irradiated with the Fish Canyon sanidine monitor standard in the Cd-lined in-core facility (CLICIT) at the Oregon State reactor. Ages were calculated relative to a Fish Canyon age of 28.02 Ma [Renne PR, *et al.* (1998) Intercalibration of standards, absolute ages and uncertainties in 40Ar/39Ar dating. *Chem Geol* 145:117–152]; age probability spectrum is shown below (Fig. S1). Single-step laser fusion $^{40}Ar/^{39}Ar$ analyses for individual grains were processed at the Lamont–Doherty Earth Observatory Argon Geochronology Laboratory using a CO_2 laser. Ages were calculated from Ar isotope ratios corrected for mass discrimination, interfering nuclear reactions, procedural blanks, and atmospheric Ar contamination. *J* parameter error is based on analyses of Fish Canyon standard, but error does not include uncertainty in Fish Canyon age [Renne PR, *et al.* (1998) Intercalibration of standards, absolute ages and uncertainties in 40Ar/39Ar dating. *Chem Geol* 145:117–152]. All crystals: 14.14 ± 0.05, MSWD = 5.23. Filtered (italicized crystals omitted): 14.07 ± 0.05, MSWD = 2.08, elimination criterion = 3 standard deviations.

Table S2. Mount Boreas site sediment carbon analyses

Sample no.	Description	$\delta^{13}C$	% C	% N	C/N
05-21A	Fluvial 1	−23.7			
05-21C	Fluvial 3	−26.2			
05-21D	Fluvial 4	−26.6			
05-21E	Fluvial 5	−25.7			
05-21F	Fluvial 5	−23.3			
05-21G	Fluvial 5	−21.8			
05-21H	Lacustrine 1	−23.5	1.9	0.1	13.9
05-21I	Lacustrine 2	−25.0	2.6	0.2	14.2
05-21J	Lacustrine 2	−24.7	2.1	0.2	12.5
05-21K	Lacustrine 2	−24.3	1.6	0.1	11.6
05-21L	Lacustrine 4	−23.5	3.3	0.2	22.2
05-21M	Lacustrine 5	−23.1	2.2	0.2	12.8
05-21N	Lacustrine 5	−19.0	0.6	0.1	9.8
05-21O	Lacustrine 6	−23.0			
05-21P	Lacustrine 6	−19.2			
05-21Q	Lacustrine 6	−25.4			
05-21R	Lacustrine 6	−24.6			
05-21S	Lacustrine 6	−26.6			
05-21T	Lacustrine 6	−22.1			

Numbered beds in the second column refer to the numbered beds displayed in Fig. 2. Analyses were conducted at the NERC Isotope Geosciences Laboratory, Kingsley Dunham Centre, Keyworth, Nottingham NG12 5GG, United Kingdom. $^{13}C/^{12}C$ analyses were performed by combustion in a Carlo Erba NA1500 on-line to a VG Optima dual-inlet mass spectrometer with $\delta^{13}C$ values calculated to the VPDB scale. Percent C values were determined simultaneously by reference to an internal standard from the mean (shown in red) excluded from the age calculation.